Bioactive near-infrared II clusters for 3D imaging and acute inflammation inhibition

August 27 2023, by Thamarasee Jeewandara

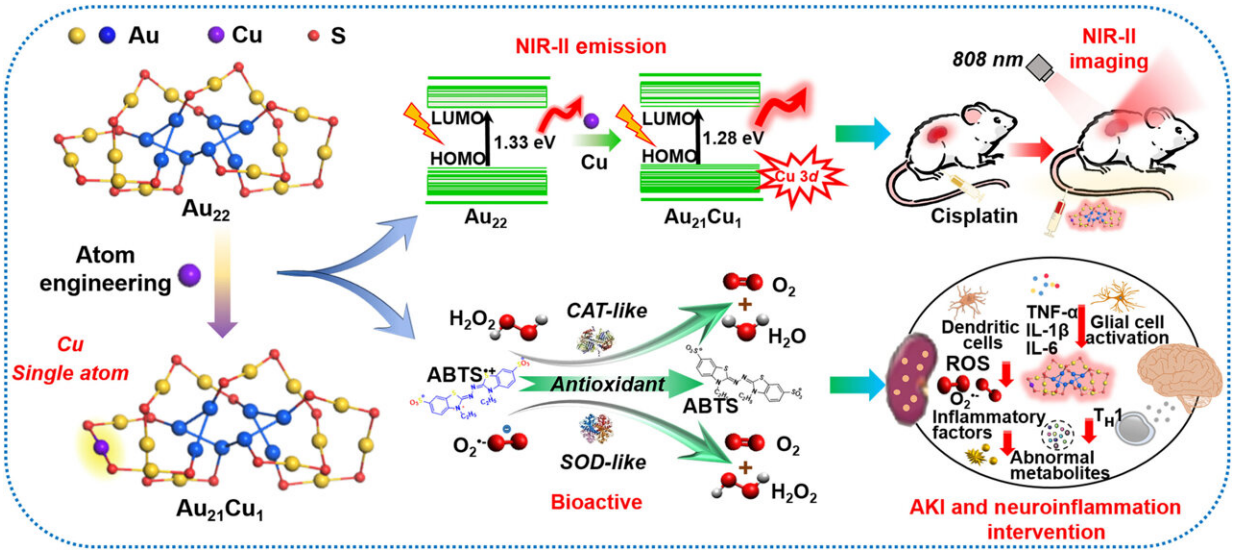

Schematic diagram of the properties and biomedical applications of Au22 clusters. We introduced Cu single-atom active sites to the atomic-precision Au22 clusters having strong NIR-II fluorescence. This atom engineering procedure reduces the bandgap from 1.33 to 1.28 eV via contributions of Cu s and p states, and Cu atom with lost electron states contributes to potent enzyme-mimicking activities. Consequently, the bioactive NIR-II clusters exhibit good capacities for highly accurate monitoring of cisplatin-induced kidney injury and inhibition of oxidative stress and inflammation in multiple organs of the cisplatin-treated mouse model, particularly in the kidneys and brain. Credit: *Science Advances*, doi: 10.1126/sciadv.adh7828

The bioactivity of most near-infrared II (NIRII) fluorophores are limited, thereby conflicting the achievement of strong fluorescence and high catalytic activities, due to a lack of free electrons in the method.

To overcome this challenge, Huizhen Ma and a research team in translational medicine, neural engineering, physics, and materials at the Tianjin University China developed atomically precise gold clusters with strong near-infrared II fluorescence to show potent enzyme-mimetic activities by using atomic engineering, to form active copper single-atom sites.

These gold-copper clusters ($Au_{21}Cu_1$) showed higher antioxidant nature with a 90-fold catalase-like and 3-fold higher superoxide dismutase-like activity compared to gold clusters alone. These clusters can be cleared through the kidney to monitor cisplatin-induced renal injury within a 20–120-minute window to visualize the process in 3D via near-infrared light-sheet microscopy.

The clusters prevented oxidative stress and inflammation in the kidney and the brain in a mouse model, which occurred as side-effects when treated with the anticancer drug cisplatin. The research is published in the journal *Science Advances*.

Monitoring the pathological evolution of oxidative-stress and inflammation in real-time

The method of near-infrared II (NIR-II) imaging offers high tissue penetration depth and signal-to-noise ratio to monitor the pathogenesis and pathological evolution of cancer with applications in neuroscience. The biocatalytic near-infrared II molecular agent is applicable to conduct real-time monitoring of pathological processes and molecular mechanisms of treatment.

Most oxidative stress-based diseases require early intervention to monitor pathological evolution in real-time. Biologists have conventionally relied on non-invasive imaging methods such as computed tomography and magnetic resonance imaging to achieve precise diagnostics and real-time analysis.

Oxidative stress and inflammation-related pathologies are however, common in clinics, necessitating real-time monitoring and intervention. Additionally, some chemotherapeutic agents often cause injury to normal tissues during medical treatment. For example, the anticancer drug cisplatin can crosslink DNA and induce oxidative stress and inflammation to result in neurotoxicity and nephrotoxicity.

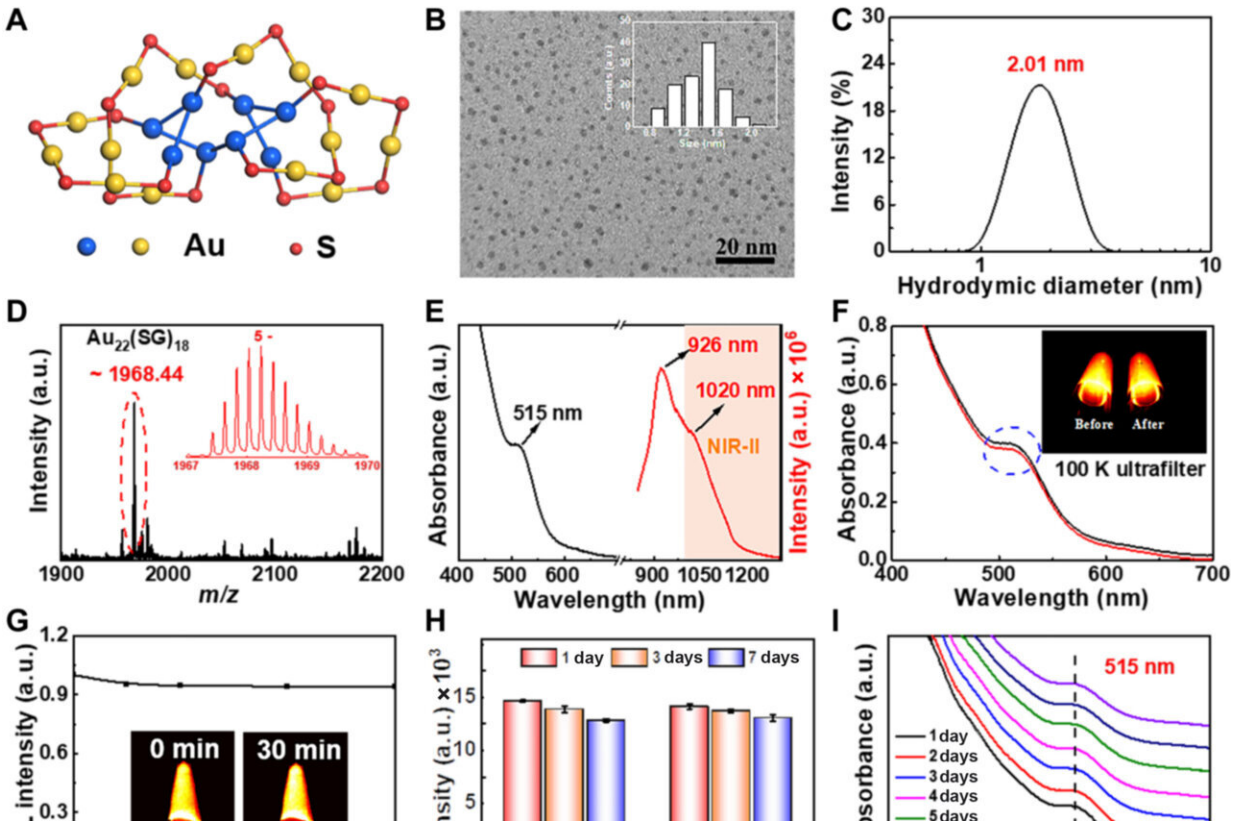

Structural characterization of gold clusters. (A) The structure illustration of Au22. Both blue and yellow represent Au atoms, and red represents S atoms. (B)

Typical TEM image of Au22 clusters with an average size of 1.5 nm. (C) The hydrodynamic size was measured to be 2.01 nm using DLS. (D) The ESI-MS of Au22 clusters. The illustration shows the molecular weight of Au22 in the m/z range from 1967 to 1970. (E) Ultraviolet-visible (UV-vis) absorption spectra and emission spectra of Au22 clusters. The black line represents the absorption spectrum, and the red line represents the emission spectrum. (F) UV-vis absorption spectra and NIR-II fluorescence images of Au22 cluster aqueous solution excited at 808 nm before and after filtration with the 100 K ultrafiltration tube (illustration: 1000 nm long pass filter, 100 ms). (G) Photostability of Au22 clusters excited with an 808 nm laser for 30 min. (H) NIR-II fluorescence stability of Au22 clusters in DI water and PBS before and after a week. (I) Stability of optical characteristic absorption peaks of Au22 clusters of 7 days in water. (J) Au 4f region of Au22 and Au21Cu1 clusters. (K) Cu 2p XPS spectrum of Au21Cu1 clusters. (L) Fourier-transformed magnitude of the Cu K-edge EXAFS spectra of Au21Cu1 and Cu foil, showing the radial distance of Cu-S bond and Cu-Cu bond. Credit: Science Advances, doi: 10.1126/sciadv.adh7828

Cisplatin-induced acute kidney injury is a common side-effect that can cause a sudden decrease in kidney function within a few hours or days. Acute kidney injury must be monitored in real-time for early diagnosis and early intervention to prevent oxidative stress and acute inflammation.

It is desirable to engineer biocatalytic NIR-II molecular agents for real-time monitoring, to synchronously achieve the inhibition of oxidative stress and early inflammation. In this work, Ma et al. developed atomic precision gold clusters with NIR-II emersion and bioactive enzyme mimicry to inhibit oxidative stress and inflammation in the injured kidney and brain.

Doping gold clusters

The team prepared gold clusters (Au_{22}) and purified them according to previous reports to create a stable structure, which they examined using transmission electron microscopy to reveal an ultrasmall size.

This allowed for efficient clearance during renal filtration. The gold clusters showed excellent photostability to reveal well-defined atomic precision engineering, water solubility, and a stable structure suited for further applications.

The team also included atomic engineering to modify gold clusters with various other metallic elements to obtain optical absorption spectra of the doped clusters. The outcomes highlighted gold-copper clusters to possess good homogeneity and dispersion, consistent with gold clusters alone.

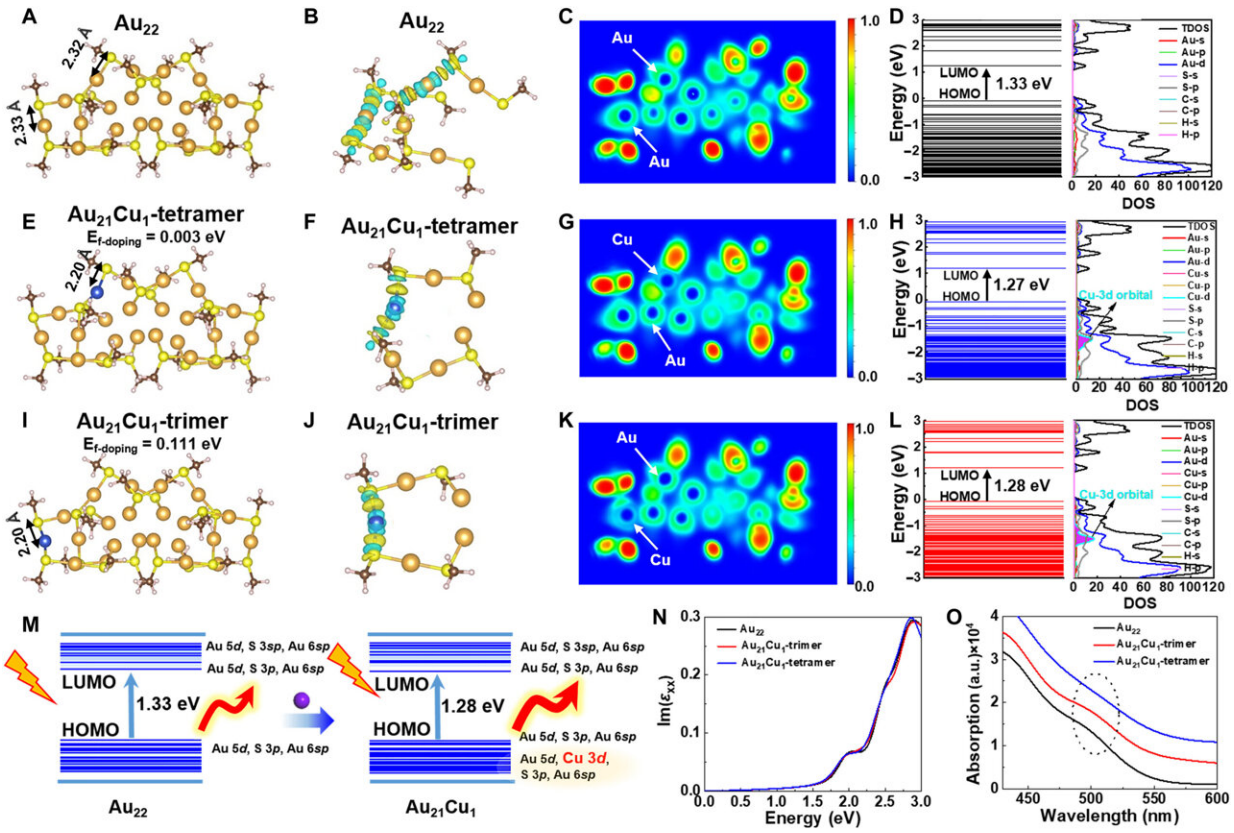

DFT calculations of gold clusters. The geometrically optimized structures of (A) Au22, (E) Au21Cu1-tetramer, and (I) Au21Cu1-trimer clusters. Orange, yellow, and blue balls represent Au, S, and Cu atoms, respectively. The locally enlarged version of charge density difference of (B) Au22, (F), Au21Cu1-tetramer, and (J) Au21Cu1-trimer clusters. The ELF images of (C) Au22, (G) Au21Cu1-tetramer, and (K) Au21Cu1-trimer clusters. The energy levels of (D) Au22, (H) Au21Cu1-tetramer, and (L) Au21Cu1-trimer clusters were simulated by density DFT. (M) The energy level diagram of Au22 and Au21Cu1 clusters. (N) The imaginary part of the dielectric function ε2 (ω). (O) The absorption spectra of the Au22, Au21Cu1-tetramer, and Au21Cu1-trimer system. Credit: Science Advances, doi: 10.1126/sciadv.adh7828

Enzymatic properties of gold clusters

The gold-copper clusters containing a single copper atom active site showed high catalytic activity. The researchers further assessed the reactive oxygen and nitrogen species absorption capacity on the molecules. The catalytic activity of the doped clusters were 90 times higher than of the pure gold alone.

This work also highlighted the impact of clusters with NIR-II properties in detail for the first time, as it plays a key role in the life sciences. The bioengineered bioactive NIR-II molecules also provided an urgent and significant platform to understand the mechanism. Ma et al. followed these experiments with density functional theory calculations of gold clusters.

Monitoring the kidney in real-time

The scientists next examined the impact of gold clusters for real-time kidney monitoring to examine kidney injury on mice in advance of

clinical diagnosis. To accomplish this, they administered the anticancer drug cisplatin to mice via injection, the outcomes highlighted severe impairment of kidney function and influence on the nervous system upon cisplatin injection, where the filtering effect of the glomeruli weakened to accumulate gold clusters in the kidney.

The team conducted cytotoxicity tests to pinpoint the region of enzymatic biological activity of the clusters by monitoring proximal tubular cells and mouse microglia. The outcomes showed the capacity of the clusters to regulate oxidative stress and induce favorable biological activities without toxicity at high concentrations.

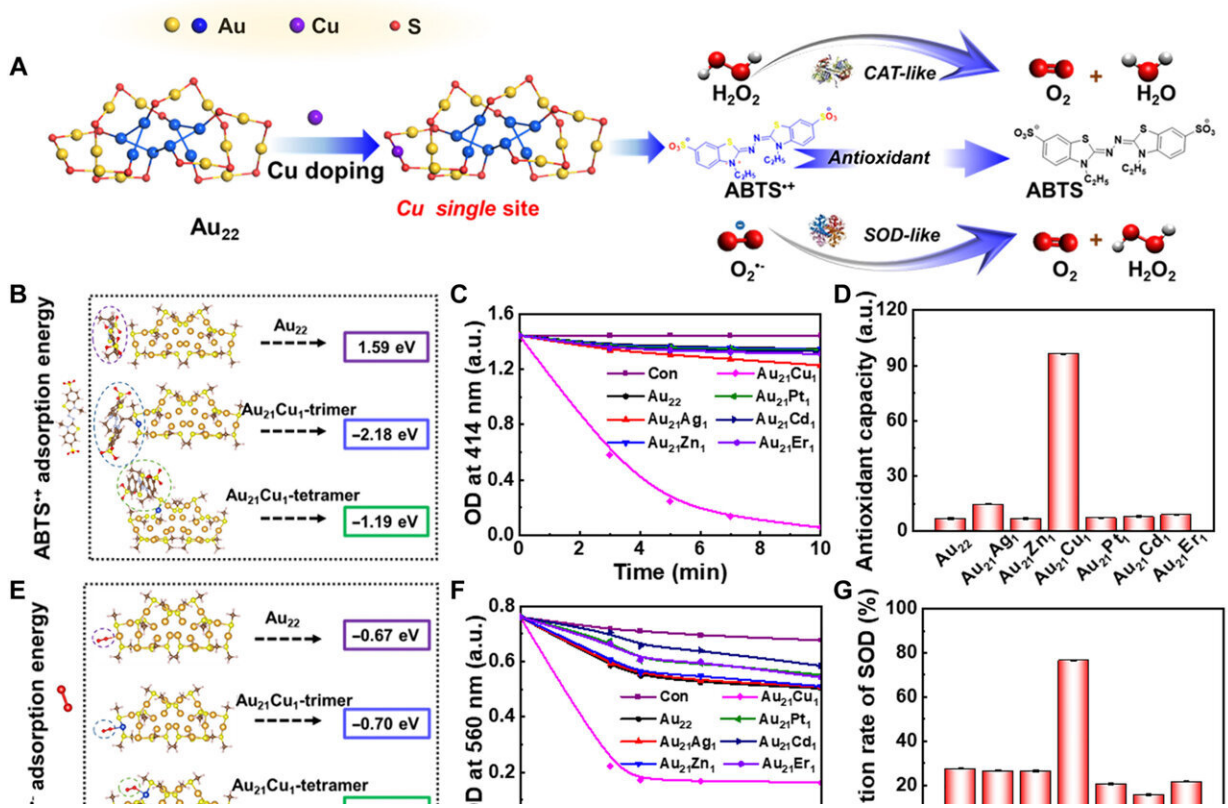

The enzyme-mimicking activity of gold clusters. (A) Schematic illustration of the enzyme-mimicking activity of Au22 clusters. (B) The adsorption energy of ABTS•+ on Au22, Au21Cu1-trimer, and Au21Cu1-tetramer clusters,

respectively. Time-dependent curves (C) and quantitative results (D) of ABTS•+ of Au22 and Au21M1 (M: Ag, Zn, Cu, Pt, Cd, and Er) clusters. (E) The adsorption energy of O2•− on Au22, Au21Cu1-trimer, and Au21Cu1-tetramer clusters, respectively. Time-dependent curves (F) and quantitative results (G) of O2•− of Au22 and Au21M1 clusters. (H) The adsorption energy of H2O2 on Au22, Au21Cu1-trimer, and Au21Cu1-tetramer clusters, respectively. Diagram (I) and quantitative results (J) of the CAT-like activity of Au22 and Au21M1 clusters. (K) The adsorption energy of ONOO− on Au22, Au21Cu1-trimer, and Au21Cu1-tetramer clusters, respectively. Time-dependent curves (L) and quantitative results (M) of ONOO− of Au22 and Au21M1 clusters. Credit: Science Advances, doi: 10.1126/sciadv.adh7828

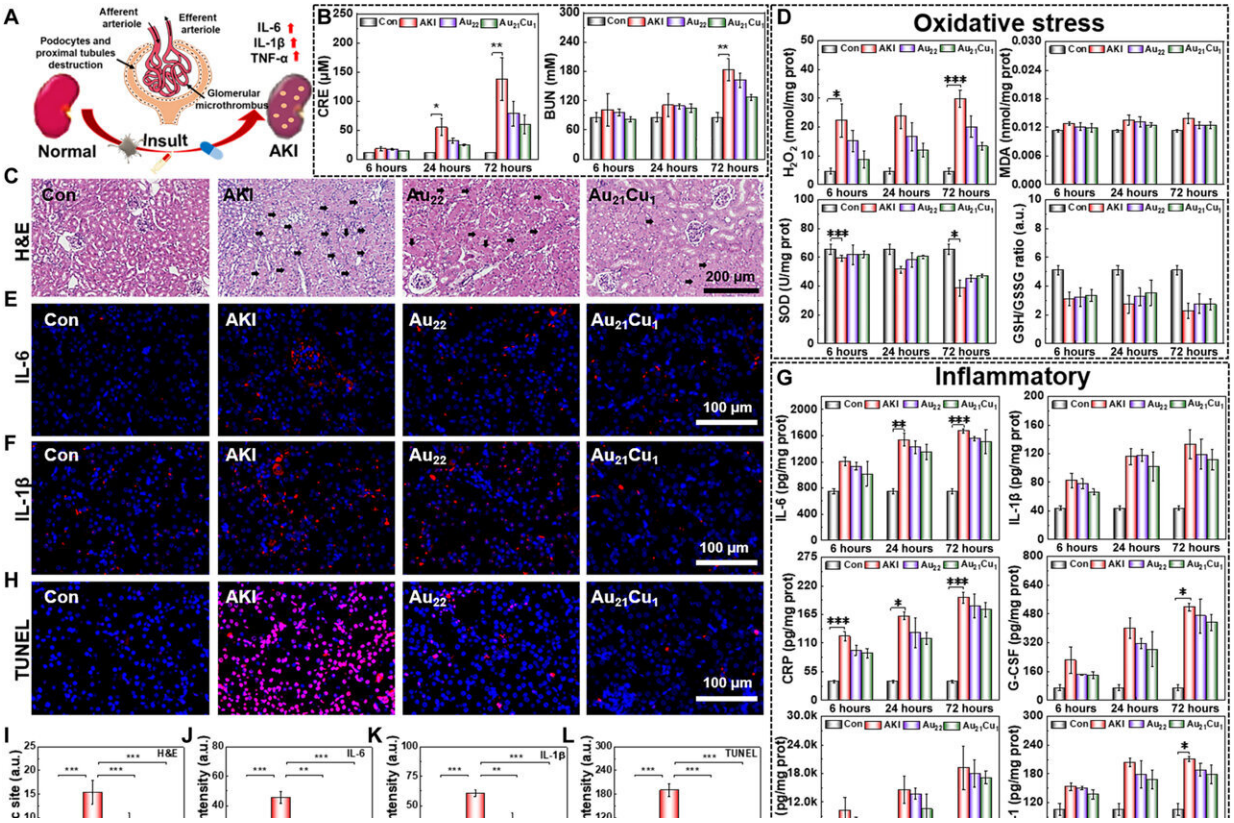

In vitro treatment of cisplatin-induced AKI with gold clusters. (A) Schematic diagram of cellular level experiments. HK2 cell viability in the presence of cisplatin with or without treatment of Au22 clusters (B) and Au21Cu1 (C)

determined by CCK8 assays (n = 3 per group). BV2 cell viability in the presence of cisplatin with or without treatment of Au22 clusters (D) and Au21Cu1 (E) determined by CCK8 assays (n = 3 per group). (F) Fluorescence microscopic images of intracellular ROS and O2•− levels induced by cisplatin with or without gold clusters. Quantitative analysis of ROS (G) and O2•− (H) fluorescence intensity (n = 3 per group). (I to K) Fluorescence quantification of HK2 cells staining for ROS and O2•− by flow cytometry (n = 3 per group). (L to N) Fluorescence-activated cell sorting (FACS) results and fluorescence quantification of BV2 cells staining for ROS and O2•− by flow cytometry (n = 3 per group). The level of TNF-α in the cellular supernatant of HK2 cells (O) and BV2 cells (P) (n = 2 per group). (Q) Representative fluorescence image of TLR4 in HK2 cells. (R) Quantitative analysis of TLR4 fluorescence intensity. Data are presented as means ± SD; *P

Ma and colleagues studied the regulation of oxidative stress and inflammation induced by cisplatin. While cisplatin is an anticancer drug, it is limited by strong side-effects relative to nephrotoxicity and ischemic injury. The association with severe reactive oxygen species and inflammation leads to mortality and comorbidities in the brain.

This can be diagnosed in advance by monitoring serum creatinine and blood urea nitrogen; clinical manifestations of nitrogenous waste buildup that provide effective indices of kidney excretory function.

Outlook

In this way, Huizhen Ma and colleagues detailed atomic engineering of gold-copper clusters where a single copper atom allowed ultrahigh enzymatic mimicry. The antioxidant activity of the gold clusters were increased by introducing copper and the biological experiments showed capacity to inhibit both oxidation stress and inflammation in the kidney-brain axis during kidney disease.

The clusters also underwent effective renal clearance and revealed non-toxicity at a high dose, to provide a compound with efficient biosafety and

multifunctionality, coupled with near-infrared II fluorescence. The gold clusters showed great potential for real-time imaging and early intervention during acute kidney injury with promising impact from the lab to clinical translation.

More information: Huizhen Ma et al, Bioactive NIR-II gold clusters for three-dimensional imaging and acute inflammation inhibition, *Science Advances* (2023). DOI: 10.1126/sciadv.adh7828

Peng Pei et al, X-ray-activated persistent luminescence nanomaterials for NIR-II imaging, *Nature Nanotechnology* (2021). DOI: 10.1038/s41565-021-00922-3